

## Entropy and efficiency in laser cooling of solids

X. L. Ruan,<sup>1,\*</sup> S. C. Rand,<sup>2</sup> and M. Kaviani<sup>1,†</sup>

<sup>1</sup>*Department of Mechanical Engineering, University of Michigan, Ann Arbor, Michigan 48105, USA*

<sup>2</sup>*Department of Electrical Engineering and Computer Science, University of Michigan, Ann Arbor, Michigan 48105, USA*

(Received 19 April 2006; revised manuscript received 25 April 2007; published 18 June 2007)

The thermodynamics of laser cooling of solids is analyzed. Using the general theory of radiation entropy, the important roles of the optical frequency and the photon distribution function in determining the radiation entropy are identified. The usefulness of a narrow-band approximation is established for a wide range of radiant sources. This approximation is then applied to compare the entropies of different light sources, including blackbody radiation, lasers, fluorescence, and the emerging class of random lasers. Based on these results, the Carnot efficiency for laser cooling of solids is determined for emission fields with various entropy characteristics. It is shown that fluorescent emission is the most efficient form of the radiated field for laser cooling of solids, and cooling schemes based on any stimulated emission process (including random laser action) are inherently less efficient. The influence of luminescence quantum yield on cooling is also considered.

DOI: [10.1103/PhysRevB.75.214304](https://doi.org/10.1103/PhysRevB.75.214304)

PACS number(s): 42.55.-f, 05.70.Ln, 78.70.-g

### I. INTRODUCTION

As formulated by Boltzmann,<sup>1</sup> thermodynamic entropy is determined by simply counting the number of available states associated with specified degrees of freedom of a system. However it is closely related to numerous other properties of systems such as information content,<sup>2,3</sup> temperature, and perhaps even the structure of matter and space-time itself,<sup>4</sup> because the states in question can be any of a multitude of internal or external degrees of freedom of the objects of which the system is composed. Entropy analyses can therefore place stringent limits on physical processes that alter the state of matter, provided the system is not displaced too far from thermodynamic equilibrium. For example, it can describe the evolution of the kinetic temperature during slow heating or cooling. In this paper, entropy calculations are used to calculate the effects of various light sources and re-emission processes on the cooling of condensed matter by radiation in order to assess their comparative efficacy, by explicitly accounting for entropy content of the radiation fields. Just as for laser cooling of gases,<sup>5</sup> spontaneous emission is shown to be important in mediating the irreversibility needed for laser cooling of solids using very general arguments.

The concept of optical refrigeration dates back to 1929, when Pringsheim recognized that thermal energy associated with the translational degrees of freedom of isolated atoms could be reduced by the process of anti-Stokes fluorescence.<sup>6</sup> In this process, absorption of the red detuned beam occurs when some fluctuation in the configuration of the atomic positions in the solid permits it by lowering some electronic energy level. Subsequent reequilibration raises the atomic energy level and lowers the total vibrational energy remaining, as shown in Fig. 1. As a result, the system loses an amount of energy equal to the frequency detuning multiplied by Planck's constant, every time a quantum is absorbed and the atom emits a photon. In gases it is important that this mechanism is consistent with a net loss of momentum because on average atoms moving toward the source present a higher probability for light absorption and are slowed by

momentum transfer during the interaction. The average energy in a single translational degree of freedom is thereby reduced. One may refer to this as a reduced, one-dimensional kinetic temperature defined by  $\frac{1}{2}k_B T = \langle E_k \rangle$ , although the velocity distribution is not likely to be Maxwellian in the presence of light, and the one-dimensional distribution might readily be different from the three-dimensional distribution that defines the equilibrium temperature.<sup>5</sup> In solids, although free translational motion of atoms does not take place, anti-Stokes fluorescence is also known to occur.<sup>7</sup>

Historically, it was believed at first that optical cooling by anti-Stokes fluorescence contradicted the second law of thermodynamics. Predictions suggested that the cycle of excitation and fluorescence was reversible, but that optical cooling would require the transformation of heat into work.<sup>8,9</sup> This issue was cleared up by Landau, who pointed out that entropy must be assigned to the radiation field<sup>10</sup> for a consistent description. Entropy of the radiation field was shown to be proportional to the frequency bandwidth and also to the solid angle of the propagating light. Typically, lasers have very small bandwidths and are highly directional, so their entropy is low. On the other hand, spontaneous fluorescence tends to

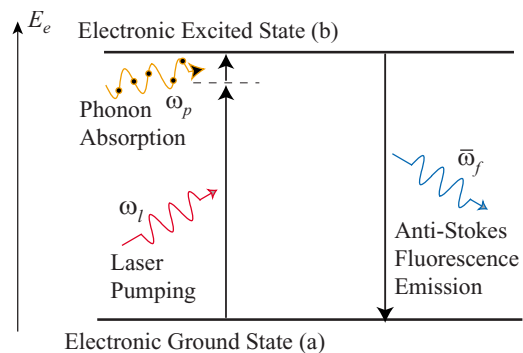


FIG. 1. (Color online) The principle of laser cooling in rare-earth ion doped crystal. The electron is excited by absorbing a laser pumping photon and one or more lattice phonons, and then decays by emitting a higher energy fluorescence photon. The dashed level is a vibrational sublevel.

be broadband and is emitted in all directions. Consequently its entropy is comparatively high. A consistent description of optical cooling must include the entropy of the incident and outgoing radiation fields.

In the present paper the theoretical cooling efficiencies achievable with ideal laser input and various output light fields are calculated and compared. First, the general theory of radiation entropy is reviewed, and a narrow-band approximation is justified to simplify the entropy calculation. Based on this approximation, the entropies for a variety of representative light fields are calculated and compared. Then, it is assumed that a single mode laser is used to irradiate a solid whose emission covers the range from broadband spontaneous emission to random laser or diode laser output. Laser cooling efficiencies are then calculated versus the photon distribution function, which describes the character of the output field. In this way it is shown that single mode excitation and fluorescent output optimize the laser cooling process in solids just as in gases, whereas stimulated emission output invariably lowers the cooling efficiency.

## II. RADIATION ENTROPY

The total power  $P$  of a steady, unpolarized beam of light (not necessarily collimated) crossing a surface  $A$ , that lies in the  $x$ - $y$  plane perpendicular to the direction  $z$  of propagation, is given by the integral of the spectral radiance  $K_\omega$  over frequency and solid angle.<sup>11</sup> That is,

$$P = \int_A \int_\Omega \int_\omega K_\omega d\omega \cos \theta d\Omega dA, \quad (1)$$

where  $\omega$  is the optical frequency,  $\Omega$  is the solid angle, and  $\theta$  is the polar angle between the surface normal and the  $z$  axis. The spectral radiance  $K_\omega$ , which is the energy per unit time, area, angular frequency, and solid angle, is related to the light source characteristics by

$$K_\omega = (\hbar\omega)c \frac{D(\omega)n}{4\pi} = \frac{\hbar n \omega^3}{4\pi^3 c^2}. \quad (2)$$

Here  $c$  is the speed of light in vacuum,  $D(\omega)$  is the photon density of states given by  $D(\omega) = \omega^2 / (\pi^2 c^3)$ ,<sup>12</sup> and  $n$  is the photon distribution function. The spectral radiance  $K_\omega$  can be determined in practice with a spectrally dispersed measurement of the absolute intensity of the source, and then the photon distribution function  $n$  can be determined by inverting Eq. (2). The function  $n$ , which specifies how the radiant energy is distributed among available modes and frequencies, is the key quantity characterizing the nature of a light source in this paper.

In terms of  $n$ , the beam power can be written as

$$P = \frac{\hbar}{4\pi^3 c^2} \int_A \int_\Omega \int_\omega n \omega^3 d\omega \cos \theta d\Omega dA. \quad (3)$$

Finding the entropy flow rate of a light beam is not as straightforward as determining power  $P$ , since the gas of photons is not necessarily in equilibrium. Landau<sup>10</sup> was the first to assign entropy to radiation fields by applying the

Bose statistics to a ‘‘photon gas.’’ A detailed derivation of entropy for light has been given in Refs. 11, 13, and 14.

We introduce the probability  $P(N_1, N_2, \dots, N_m)$  of finding  $N_1$  photons in optical mode 1,  $N_2$  photons in mode 2,  $\dots$ , and  $N_m$  photons in mode  $m$  ( $m \geq 1$ ). Here the optical mode refers to the photon wave vector, and photons sharing the same wave vector are in the same mode. Then the entropy of the photon gas is given by<sup>1,13</sup>

$$S = -k_B \sum_{N_1} \sum_{N_2} \cdots \sum_{N_m} P(N_1, N_2, \dots, N_m) \ln P(N_1, N_2, \dots, N_m), \quad (4)$$

where  $k_B$  is the Boltzmann constant. Denoting the probability of finding  $N_j$  photons in mode  $j$  ( $j=1, 2, \dots, m$ ) by  $p_j(N_j)$ , and assuming that  $p_j(N_j)$  is independent of the occupation of other modes, the probability becomes

$$P(N_1, N_2, \dots, N_m) = p_1(N_1) p_2(N_2) \cdots p_m(N_m), \quad (5)$$

where normalization requires

$$\sum_{N_j=0}^{\infty} p_j(N_j) = 1, \quad (6)$$

for each mode  $j$ . Substituting Eq. (5) into (4), and using (6), one finds

$$S = -k_B \sum_{j=1}^m \sum_{N_j=0}^{\infty} p_j(N_j) \ln p_j(N_j) = \sum_{j=1}^m S_j, \quad (7)$$

where the partial entropy for one mode  $j$  is

$$S_j = -k_B \sum_{N_j=0}^{\infty} p_j(N_j) \ln p_j(N_j). \quad (8)$$

These equations indicate that the total entropy of a multi-mode field can be decomposed into entropies for each mode.

Next assume that the probability of finding one additional photon in any state is independent of the number already occupying that state. Thus  $p_j(N_j) \propto q_j^{N_j}$ , where  $q_j$  is a number between 0 and 1 for all light sources. For example,  $q_j = \exp(-\hbar\omega_j/k_B T)$  for blackbody emission.<sup>12</sup> The normalization requirement Eq. (6) gives

$$p_j(N_j) = q_j^{N_j} \left/ \sum_{l=0}^{\infty} q_j^l \right. = (1 - q_j) q_j^{N_j} \quad (0 \leq q_j \leq 1). \quad (9)$$

The distribution function  $n_j$  of state  $j$ , which gives the weighted occupation of the mode, can therefore be written as

$$n_j = \sum_{N_j=0}^{\infty} N_j p_j(N_j) = \sum_{N_j=0}^{\infty} N_j (1 - q_j) q_j^{N_j} = \frac{q_j}{1 - q_j}, \quad (10)$$

Substituting Eqs. (9) and (10) into (7), the entropy of the photons can be written in terms of  $n_j$  as

$$S = k_B \sum_{j=1}^m [(1 + n_j) \ln(1 + n_j) - n_j \ln n_j], \quad (11)$$

and the entropy for the mode  $j$  becomes

$$S_j = k_B[(1 + n_j)\ln(1 + n_j) - n_j \ln n_j]. \quad (12)$$

In much the same way that we have defined the spectral energy radiance  $K_\omega$ , a spectral entropy radiance  $L_\omega$  (the entropy per unit time, area, angular frequency, and solid angle) can also be defined as

$$L_\omega = S_j c \frac{D(\omega)}{4\pi} = \frac{k_B\{(1+n)\ln[(1+n)] - n \ln n\}\omega^2}{4\pi^3 c^2}. \quad (13)$$

In terms of this quantity, the entropy flow rate  $\dot{S}$  of a light beam can finally be written as

$$\dot{S} = \int_A \int_\Omega \int_\omega L_\omega d\omega \cos \theta d\Omega dA = \frac{k_B}{4\pi^3 c^2} \int_A \int_\Omega \int_\omega [(1+n)\ln(1+n) - n \ln n] \omega^2 d\omega \cos \theta d\Omega dA. \quad (14)$$

The quantity  $\dot{S}$  is suitable for characterizing the degree of disorder of a light beam. However, it is an extensive variable rather than an intensive variable. For example, if we just double the surface area of a blackbody, the entropy of its radiation is also doubled, although the radiation is essentially still of the same class. On the other hand, a high-power diode laser beam might contain the same amount of entropy as a very low-power blackbody radiation, although the nature of the radiation is very different. Hence, the amount of entropy is always dependent on the beam power, and cannot be used meaningfully on its own to distinguish or characterize various radiation fields. A more suitable parameter for this purpose is the entropy flow rate per unit power,

$$\frac{\dot{S}}{P} = \frac{k_B}{\hbar} \frac{\int_A \int_\Omega \int_\omega \{(1+n)\ln[(1+n)] - n \ln n\} \omega^2 d\omega \cos \theta d\Omega dA}{\int_A \int_\Omega \int_\omega n \omega^3 d\omega \cos \theta d\Omega dA}. \quad (15)$$

Here  $\dot{S}/P$  has units of inverse temperature ( $K^{-1}$ ), and the reciprocal of this quantity is often referred to as the “flux temperature” of the beam in the literature.<sup>11,13</sup>

The entropy flow rate per unit power  $\dot{S}/P$  covers many orders of magnitude for different radiation fields, and in the present paper represents the beam “quality.” Hence, as will be seen in Sec. V,  $\dot{S}/P$  rather than  $\dot{S}$  is an essential parameter in calculating the Carnot efficiency for laser cooling.

### III. ROLES OF ANGULAR FREQUENCY AND DISTRIBUTION FUNCTION IN RADIATION ENTROPY

Equation (15) completely describes the roles of distribution function, area, frequency, and solid angle in the entropy flow rate per unit power. However, for nonthermal (nonequilibrium) radiation with arbitrary distribution functions the calculation of  $\dot{S}/P$  is laborious. Consequently we proceed below to examine a useful approximation for the radiance based on an assumption that the radiation can be treated as “narrow-band.”

Introducing a central frequency  $\omega_0$ , frequency bandwidth  $\Delta\omega$ , and divergence angle  $\delta$  of the beam, we rewrite the power in a form that is more convenient for analysis. If the radiation is narrow-band, and isotropic within the circular cone of half-angle  $\delta$ , the power of the beam can be approximated as

$$P = \int_A \int_\Omega \int_{\Delta\omega} K_\omega \cos \theta d\omega d\Omega dA = \bar{K}_\omega A \Delta\omega \pi \sin^2 \delta, \quad (16)$$

where  $\bar{K}_\omega$  is the mean radiance over the frequency bandwidth and beam solid angle. Note that in the original spectrum the frequency runs over the interval 0 to  $\infty$ , while here, we only consider the range  $\Delta\omega$  given by the full-width at half-maximum (FWHM). This assumes that the energy and entropy outside this range can be neglected.

According to Eq. (2), an estimated or average distribution function  $\bar{n}$  can be defined that is related to the average radiance  $\bar{K}_\omega$  through

$$\bar{K}_\omega = \frac{\hbar \bar{n} \omega_0^3}{4\pi^3 c^2}. \quad (17)$$

Note that in this expression the variable  $\omega$  has been replaced with the central frequency  $\omega_0$  in the optical spectrum. In the same way that  $n$  can be calculated from  $K_\omega$  using Eq. (2), the average distribution function  $\bar{n}$  can readily be calculated from the mean radiance  $\bar{K}_\omega$  using Eq. (17).

The entropy flow rate is then approximated in a similar fashion,

$$\dot{S} = \frac{k_B}{4\pi^3 c^2} \{(1 + \bar{n})\ln[(1 + \bar{n})] - \bar{n} \ln \bar{n}\} \omega_0^2 A \Delta\omega \pi \sin^2 \delta. \quad (18)$$

Hence the entropy flow rate per unit power reduces to

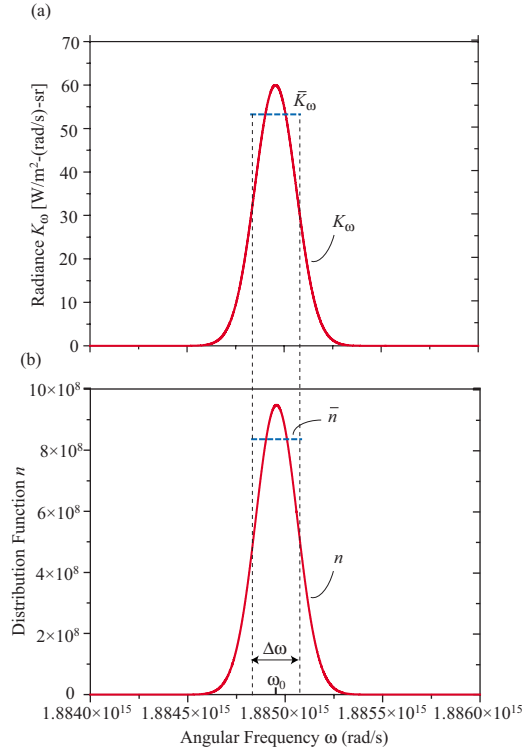


FIG. 2. (Color online) (a) The spectral radiance  $K_\omega$  (solid curve) and the average radiance  $\bar{K}_\omega$  (dashed curve), (b) the spectral distribution function  $n$  (solid curve) and the average distribution function  $\bar{n}$  (dashed curve). The central frequency is  $\omega_0 = 1.8850 \times 10^{15}$  rad/s, and the bandwidth  $\Delta\omega = 2.5133 \times 10^{11}$  rad/s.

$$\frac{\dot{S}}{P} = \frac{k_B}{\hbar\omega_0} \frac{(1 + \bar{n}) \ln[(1 + \bar{n})] - \bar{n} \ln \bar{n}}{\bar{n}}. \quad (19)$$

This expression, while being limited to narrow-band radiation, is much simpler than the general relation in Eq. (15). It has the merit of showing that for narrow-band sources the entropy flow rate per unit power is inversely proportional to the central frequency  $\omega_0$ , and is decreasing with an increasing average distribution function  $\bar{n}$ .

To investigate the applicability of the narrow-band approximation, we now compare results based on Eq. (19) with exact results based on Eq. (15). Narrow-band radiation is considered for which the spectral radiance is described by a Gaussian distribution

$$K_\omega = K_0 \exp\left[-\left(\frac{\omega - \omega_0}{\sqrt{\ln 2} \Delta\omega}\right)^2\right]. \quad (20)$$

Here  $K_0$  is the spectral radiance at the central frequency  $\omega_0$  of the source, and  $\Delta\omega$  is the spectral width. Representative values for optical sources are  $K_0 = 60$  W/m<sup>2</sup>-(rad/s)-sr,  $\omega_0 = 1.8850 \times 10^{15}$  rad/s (or the central wavelength  $\lambda_0 = 1$   $\mu$ m), and  $\Delta\omega = 2.5133 \times 10^{11}$  rad/s (or  $\Delta\lambda = 0.133$  nm). The corresponding spectral radiance  $K_\omega$  and distribution function  $f$  are shown in Figs. 2(a) and 2(b) respectively. The exact entropy flow rate per unit power, calculated using Eq. (15), is  $5.59 \times 10^{-12}$  K<sup>-1</sup>. To use the narrow-band approximation, the average radiance is first calculated using

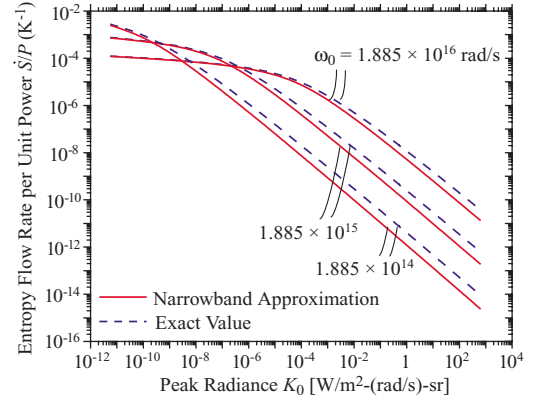


FIG. 3. (Color online) Entropy flow rate per unit power as a function of the peak radiance  $K_0$ , for a few central frequency  $\omega_0$ . The narrow-band approximation and exact results are shown, indicating convergence at low  $K_0$ .

$$\bar{K}_\omega = \frac{\int_{\Delta\omega} K_\omega d\omega}{\Delta\omega}, \quad (21)$$

and then the average distribution function is derived from it using

$$\bar{n} = \frac{4\pi^3 c^2 \bar{K}_\omega}{\hbar\omega_0^3}. \quad (22)$$

The results of the narrow-band approximation are given by the dashed curves in Figs. 2(a) and 2(b). The approximate entropy flow rate per unit power calculated using Eq. (19) is found to be  $1.79 \times 10^{-12}$  K<sup>-1</sup>. This value is only one-third of the exact value. This is an acceptable approximation in cases where no other highly ordered light source with comparable entropy is present, as explained below. For example, in laser cooling of solids considered here, we have three input and output energy flows: the laser pumping, the fluorescence emission, and the thermal load. Since the entropy of the laser pumping is orders of magnitude lower than the other two, a deviation of 3 times in its entropy will make no difference in the Carnot efficiency, as will be seen in Sec. V.

To further check the validity of the narrow-band approximation for a variety of Gaussian sources, we calculated the exact and approximate entropy flow rate per unit power  $\dot{S}/P$  over a wide range of values of  $K_0$ ,  $\omega_0$ , and  $\Delta\omega$ . Interestingly,  $\dot{S}/P$  is not a function of the bandwidth  $\Delta\omega$ , since  $\Delta\omega$  does not affect the mean distribution function  $\bar{n}$ , for a given  $K_0$  and  $\omega_0$ . Hence,  $\dot{S}/P$  is plotted only as a function of  $K_0$  and  $\omega_0$  in Fig. 3. In the figure, it is evident that the approximate results agree very well with the exact results in the low radiance region. This is because for low radiance  $\dot{S}/P$  is a weak function of  $K_0$ , while for high radiance it decreases strongly as a function of  $K_0$ . Hence the approximate approach agrees best with exact calculations at low radiance.

The narrow-band approximation also works surprisingly well for some sources of broadband radiation. We show this

by considering an additional case of the blackbody spectral radiance, which is

$$K_{\omega}^0 = \frac{\hbar}{4\pi^3 c^2} n^0 \omega^3, \quad (23)$$

with  $n^0$  being given by the equilibrium distribution function

$$n^0 = \frac{1}{e^{\hbar\omega/k_B T_b} - 1}. \quad (24)$$

This is the usual Bose-Einstein distribution, and  $T_b$  is the temperature of the cavity which emits the blackbody radiation.

Blackbody emission is a special case for which an exact analytical expression for  $\dot{S}/P$  can be obtained. As this form of radiation field is uniformly directed in space, its power  $P$  is given by Eq. (1), i.e.,

$$P = A\pi \frac{\hbar}{4\pi^3 c^2} \int_0^{\infty} n^0 \omega^3 d\omega = \sigma_{\text{SB}} A T_b^4, \quad (25)$$

where  $\sigma_{\text{SB}}$  is the Stefan-Boltzmann constant. The corresponding entropy flow rate is

$$\begin{aligned} \dot{S} &= A\pi \frac{k_B}{4\pi^3 c^2} \int_0^{\infty} \{(1+n^0)\ln[(1+n^0)] - n^0 \ln n^0\} d\omega \\ &= \frac{4}{3} \sigma_{\text{SB}} A T_b^3, \end{aligned} \quad (26)$$

with the result that the entropy flow rate per unit power is

$$\frac{\dot{S}}{P} = \frac{4}{3T_b}. \quad (27)$$

As a numerical example, consider blackbody emission from a cavity at room temperature  $T_b=300$  K. The spectral radiance and distribution function are shown in Figs. 4(a) and 4(b) respectively. The exact value of  $\dot{S}/P$ , calculated using Eq. (27), is  $\dot{S}/P=4.44 \times 10^{-3} \text{ K}^{-1}$ , while the approximate value calculated using Eq. (19) is  $4.51 \times 10^{-3} \text{ K}^{-1}$ . The difference is less than 2% and the approximation is therefore well justified in this case.

To further check the validity of this approximation for blackbody sources at a variety of temperatures of interest in this paper, we calculated the exact and approximate values of  $\dot{S}/P$  as a function of temperature. The results are plotted in Fig. 5. Interestingly, over the entire range the approximation is in excellent agreement with the exact approach, even though blackbody radiation is a broadband source. The fundamental reason behind this agreement is, in this temperature range the blackbody source has very low radiance, so that the entropy is not sensitive to any small error in  $\bar{n}$  introduced by the averaging process.

The reason the narrow-band approximation works better than expected can be understood from another perspective. In this procedure we first truncate the original spectrum and consider a restricted range of frequency  $\Delta\omega$ . This makes the approximated spectra narrower than the original ones, and *decreases* the degree of disorder. Second, this  $\Delta\omega$  range of

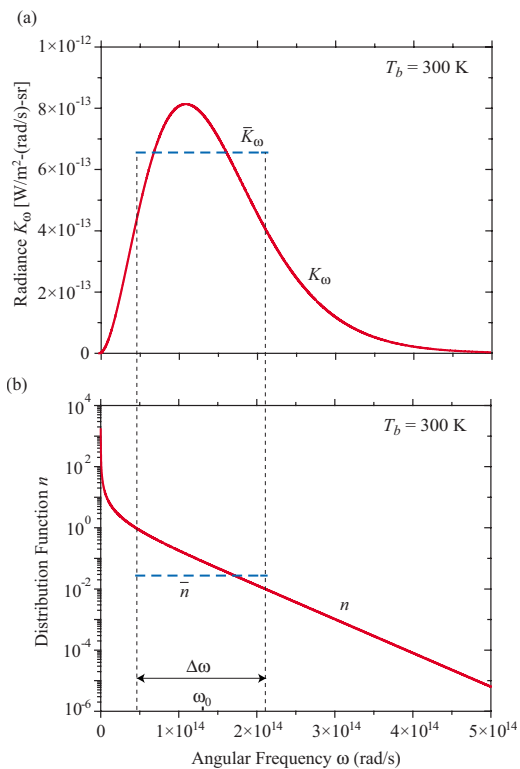


FIG. 4. (Color online) Variations of the radiance and distribution function, with respect to the angular frequency for blackbody emission at  $T_b=300$  K. The mean quantities are also shown.

the original spectra is averaged to get the mean spectra, with the result that the average radiance becomes uniformly distributed at a lower value than the peak in the original spectra. Because  $\dot{S}/P$  depends essentially inversely on  $n$ , the degree of disorder is artificially *increased* by this procedure. As a result, whether the approximate value of  $\dot{S}/P$  is found to be higher or lower than the exact value is determined by how well these two steps compensate each other. Overall, our finding is that this narrow-band approximation works particularly well for light sources of low radiance, for which  $\dot{S}/P$  is a weak function of the mean distribution function.

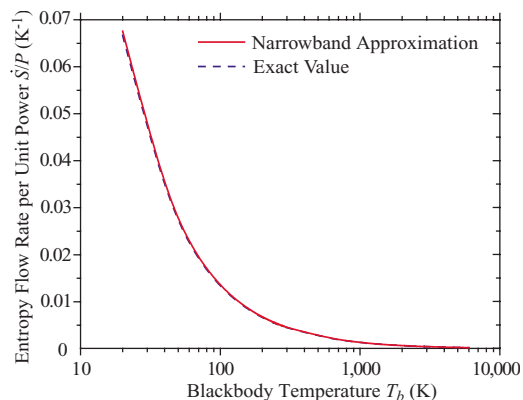


FIG. 5. (Color online) Entropy flow rate per unit power for blackbody radiation as a function of temperature. The narrow-band approximation and the exact results are shown.

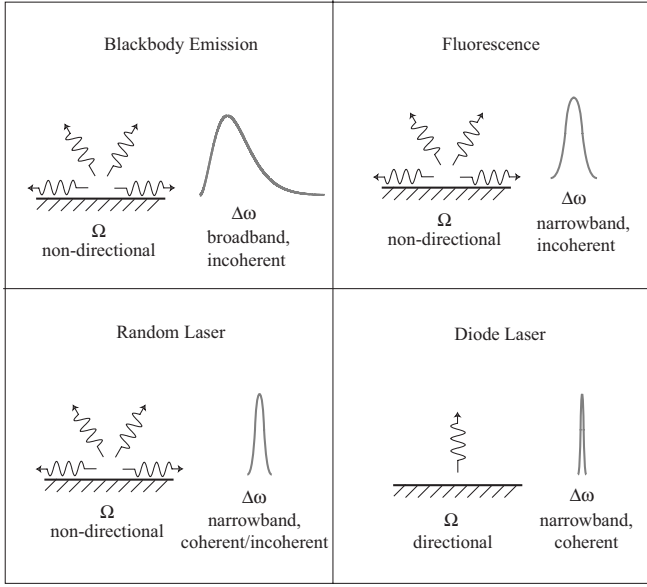


FIG. 6. Schematics of the emission bandwidth and solid angle associated with four different emission sources.

#### IV. ENTROPY OF DIFFERENT LIGHT SOURCES

A comparison of light sources with a wide variety of entropic characteristics is relevant for the evaluation of laser cooling of solids. Some sources are spectrally broadband and isotropic in space, such as blackbody sources. Some are spectrally narrow-band and directional in space, such as lasers. These cases are sketched in Fig. 6. To calculate the corresponding  $\dot{S}/P$  we only need to know the central frequency  $\omega_0$  and the average distribution function  $\bar{n}$  for each type of source. The latter can be calculated if the average spectral radiance is known, and this is facilitated by relating  $\bar{K}_\omega$  to more convenient, measurable parameters. Based on Eqs. (16) and (17), the average distribution function  $\bar{n}$  can be rewritten in terms of power  $P$ , bandwidth  $\Delta\omega$ , beam angle  $\delta$ , and central frequency  $\omega_0$ , as

$$\bar{n} = \bar{K}_\omega \frac{4\pi^3 c^2}{\hbar \omega_0^3} = \frac{P}{A \Delta\omega \pi \sin^2 \delta} \frac{4\pi^3 c^2}{\hbar \omega_0^3}. \quad (28)$$

Numerical examples for four classes of radiation fields are presented below, and the associated parameters are listed in Table I. The central wavelength  $\lambda_0$  is chosen to be the same for the purpose of comparison.

Blackbody emission has a high degree of disorder, since it is equilibrium emission from all possible electronic levels, and includes both spontaneous and stimulated emission fields. The average spectral radiance and the distribution function is determined by temperature alone. For a blackbody at  $T_b=4395$  K, the average distribution function is  $\bar{n}=0.0324$ , and the entropy flow rate per unit power is  $(\dot{S}/P)_b=3.078 \times 10^{-4} \text{ K}^{-1}$ . This is comparable to the entropy of thermal energy at this temperature, and in this sense blackbody radiation is considered as “pure heat” or “low-grade” radiation energy.<sup>11</sup>

In laser cooling of solids, the radiant output of the system is typically chosen to be fluorescence. Fluorescence is spatially isotropic spontaneous emission that is usually spectrally narrow-band. Using values relevant to laser cooling of  $\text{Yb}^{3+}:\text{ZBLANP}$  from earlier experiments,<sup>15</sup> where the central frequency and the bandwidth are  $\omega_0=2\pi c/\lambda_0=1.886 \times 10^{15} \text{ rad/s}$  (as  $\lambda_0=999.3 \text{ nm}$ ) and  $\Delta\omega=2\pi c\Delta\lambda/\lambda_0^2=5.662 \times 10^{13} \text{ rad/s}$  (as  $\Delta\lambda=35 \text{ nm}$ ), respectively, the cooling power of the system was estimated to be approximately 0.9 mW, and the corresponding fluorescence power  $P$  was 60 mW.<sup>15</sup> Assuming the fluorescence is emitted homogeneously and hemispherically out of the surface of the sample, the beam divergence is then  $\delta=\pi/2$ . The sample in Ref. 15 was a cylinder with diameter 170  $\mu\text{m}$  and length 7 mm, giving the surface area  $A=3.784 \times 10^{-6} \text{ m}^2$ . Hence the average distribution function  $\bar{n}$  was

$$\bar{n} = \frac{P}{A \pi \sin^2 \delta \Delta\omega} \frac{4\pi^3 c^2}{\hbar \omega_0^3} = 1.404 \times 10^{-3}. \quad (29)$$

This determines the entropy flow rate per unit power to be  $(\dot{S}/P)_f=5.36 \times 10^{-4} \text{ K}^{-1}$ .

TABLE I. Beam parameters and entropy flow rates per unit power for typical light sources.

	Blackbody emission ( $T_b=4,395 \text{ K}$ )	Fluorescence	Random laser	Diode laser
Beam power $P$ , W	80.05	0.06	0.06	0.06
Central wavelength $\lambda_0$ , nm	999.3	999.3	999.3	999.3
Wavelength bandwidth $\Delta\lambda$ , nm	2,223	35	1	0.1331
Central frequency $\omega_0$ , rad/s	$1.887 \times 10^{15}$	$1.887 \times 10^{15}$	$1.887 \times 10^{15}$	$1.887 \times 10^{15}$
Frequency bandwidth $\Delta\omega$ , rad/s	$2.448 \times 10^{15}$	$5.666 \times 10^{13}$	$1.888 \times 10^{12}$	$2.513 \times 10^{11}$
Surface area $A$ , $\text{m}^2$	$3.784 \times 10^{-6}$	$3.784 \times 10^{-6}$	$3.784 \times 10^{-6}$	$7.854 \times 10^{-9}$
Beam divergence $\delta$ , rad	$\pi/2$	$\pi/2$	$\pi/2$	0.001
Average radiance $\bar{K}_\omega$ , $\text{W}/\text{m}^2\text{-(rad/s)-sr}$	$2.071 \times 10^{-9}$	$8.908 \times 10^{-11}$	$2.672 \times 10^{-9}$	9.6763
Average distribution function $\bar{n}$ ,	0.0324	$1.404 \times 10^{-3}$	0.0421	$1.525 \times 10^8$
Entropy flow rate per unit power $\dot{S}/P$ , $\text{K}^{-1}$	$3.078 \times 10^{-4}$	$5.362 \times 10^{-4}$	$2.906 \times 10^{-4}$	$9.030 \times 10^{-12}$

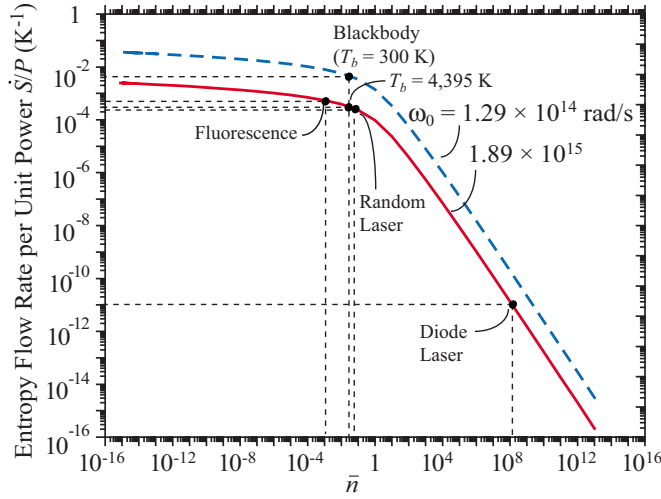


FIG. 7. (Color online) Variation of the entropy flow rate per unit volume as a function of the average distribution function  $\bar{n}$  and central frequency  $\omega_0$ , which characterizes different light sources.

In powder laser samples pumped with high intensity, random laser output with the same energy can be achieved. Emission may be considered to be homogeneous into the half-space above the emitting surface. Assuming a bandwidth of  $\Delta\lambda=1$  nm,<sup>16,17</sup> which is much narrower than that of the fluorescence, one finds  $\bar{n}=0.0421$ , and  $(\dot{S}/P)_{fl}=2.906 \times 10^{-4} \text{ K}^{-1}$ .

If the output radiation field were to be in the form of a diode laser, again operating at 60 mW with a central wavelength of 999.3 nm, but with a typical beam size of 100  $\mu\text{m}$  at the source, a bandwidth of 40 GHz and a divergence of  $\delta=1$  mrad, one would find  $\bar{n}=1.525 \times 10^8$  and  $(\dot{S}/P)_{dl}=9.03 \times 10^{-12} \text{ K}^{-1}$ .

These results for the entropy flow rate per unit power for various light sources are compared in Fig. 7. It is evident from the figure that  $\dot{S}/P$  decreases rapidly with decreasing beam bandwidth and divergence. If either the bandwidth  $\Delta\omega$  or the divergence  $\delta$  of the source drops to nearly zero, then we see from Eq. (18) that  $\dot{S}/P$  becomes

$$\dot{S} \approx \lim_{\bar{n} \rightarrow \infty} \frac{k_B A}{4\pi^2 c^2} [(1 + \bar{n}) \ln \bar{n} - \bar{n} \ln \bar{n}] \omega_0^2 \Delta\omega \sin^2 \delta = 0. \quad (30)$$

Hence the limiting case of monochromatic or unidirectional radiation (which is highly ordered) constitutes a source that carries essentially no entropy.

## V. CARNOT COOLING EFFICIENCY VERSUS EMISSION ENTROPY

Now consider a control volume that is to be cooled radiatively. This volume is labelled ‘‘optical refrigerator’’ in Fig. 8. The power flow in and out of this region reflects the balance of the pump laser, the external thermal load, and the fluorescence emission.

According to the first law of thermodynamics, we have

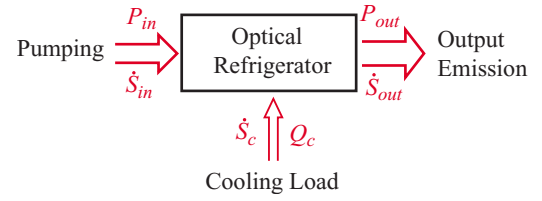


FIG. 8. (Color online) A control volume showing various input and output processes that control the energy balance during laser cooling of a solid.

$$P_{\text{out}} = P_{\text{in}} + Q_c. \quad (31)$$

The cooling efficiency is defined in the customary way for a refrigerator,<sup>18</sup> namely

$$\eta = \frac{Q_c}{P_{\text{in}}}. \quad (32)$$

The maximum value of  $\eta$  is the Carnot limit  $\eta_c$  determined by the second law of thermodynamics. The entropy carried by the fluorescence cannot be less than the sum of the entropy withdrawn from the cooling sample and the entropy transported in by the pump laser. That is,

$$\dot{S}_{\text{out}} \geq \dot{S}_{\text{in}} + \dot{S}_c, \quad (33)$$

where  $\dot{S}_{\text{in}}$ ,  $\dot{S}_{\text{out}}$ , and  $\dot{S}_c$  are the entropy flow rates for the absorbed irradiation, the output emission, and the thermal load. This equation can also be written as

$$P_{\text{out}} \left( \frac{\dot{S}}{P} \right)_{\text{out}} \geq P_{\text{in}} \left( \frac{\dot{S}}{P} \right)_{\text{in}} + \frac{Q_c}{T}, \quad (34)$$

where  $T$  is the temperature of the thermal load. The reversible Carnot limit is obtained by choosing the equality sign in Eq. (34). By substituting Eqs. (31) and (32) into Eq. (34) to eliminate  $P_{\text{in}}$ ,  $P_{\text{out}}$ , and  $Q_c$ , we find the Carnot efficiency to be

$$\eta_c = \frac{[(\dot{S}/P)_{\text{out}} - (\dot{S}/P)_{\text{in}}]T}{1 - (\dot{S}/P)_{\text{out}}T}. \quad (35)$$

Thus the cooling power and the total output power are

$$Q_c = \eta_c P_{\text{in}} \quad (36)$$

and

$$P_{\text{out}} = (1 + \eta_c) P_{\text{in}}. \quad (37)$$

Equation (35) indicates that small  $(\dot{S}/P)_{\text{in}}$  and large  $(\dot{S}/P)_{\text{out}}$  are desirable to enhance  $\eta_c$ , and that it is important to control the characteristics of both the input and output fields. A pumping source with the smallest possible  $(\dot{S}/P)_{\text{in}}$ , corresponding to a monochromatic, unidirectional, single-mode laser, is desired since  $(\dot{S}/P)_{\text{in}}=0$ . The emitted field could be in the form of fluorescence, random laser emission, or monomode laser quality emission, via appropriate selections of pumping level, sample, and feedback structures. It is therefore useful to know how the cooling efficiency can be

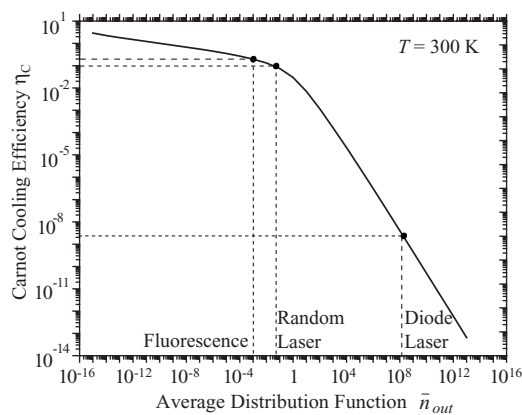


FIG. 9. Variation of the Carnot efficiency with respect to the average distribution function for the output emission fields. Three typical emission fields are marked.

influenced by controlling the radiation character of the emission fields. Under the condition of single-mode laser pumping, Eq. (35) becomes

$$\eta_c = \frac{(\dot{S}/P)_{\text{out}} T}{1 - (\dot{S}/P)_{\text{out}} T}. \quad (38)$$

Using Eq. (38), the Carnot efficiency can be calculated as a function of the entropy flow rate per unit power, or as a function of the average distribution function. The result is shown in Fig. 9. This figure indicates that fluorescent systems have the highest cooling efficiency. In the example of laser cooling of  $\text{Yb}^{3+}:\text{ZBLANP}$  discussed earlier,<sup>11</sup> the entropy flow rate per unit power of the fluorescence emission was found to be  $(\dot{S}/P)_{\text{out}} = 5.36 \times 10^{-4} \text{ K}^{-1}$ . Correspondingly, the Carnot efficiency of this optical cooler is found to be about 20% at room temperature. If stimulated emission is employed in the system, the Carnot cooling efficiency is lower. One finds  $\eta = 0.11$  for random laser emission and  $\eta = 2.7 \times 10^{-9}$  for diode laser emission, respectively. Fields of this nature are far less efficient than fluorescence emission.

Also using Eq. (38), the cooling efficiency as a function of temperature is shown in Fig. 10, for  $(\dot{S}/P)_{\text{out}} = 5.36 \times 10^{-4} \text{ K}^{-1}$ . It diminishes approximately linearly to zero as  $T \rightarrow 0$ . Note that here we do not include the dependence of  $(\dot{S}/P)_{\text{out}}$  on the fluorescence power and sample temperature, since there are not sufficient experimental data to make these calculations. When these effects are included, the cooling efficiency is still expected to diminish to zero, but at a slightly different rate.

## VI. COOLING EFFICIENCY FOR REAL SYSTEMS INCLUDING LUMINESCENCE QUANTUM YIELD

In real systems, the luminescence quantum yield is less than unity, and the energy loss during any internal relaxation process is irreversible, from a thermodynamic point of view. When considering such losses caused by nonradiative decay, it is helpful to account for the associated heat load explicitly

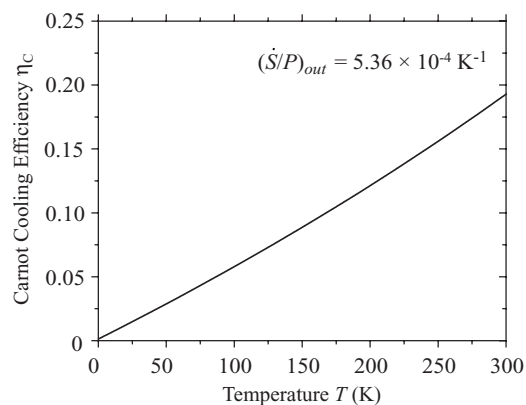


FIG. 10. Optimum Carnot efficiency as a function of temperature.

by dividing the cooling load channel shown earlier in Fig. 8 into two parts. In Fig. 11 the cooling load channel is now considered to be the reversible part of the refrigerator cycle. No entropy is generated, and the cooling load is still given by Eq. (36). In the figure, the new heat generation channel corresponds to the irreversible losses from internal relaxation, and the entropy production for this channel, also for the entire cooling cycle, is

$$\begin{aligned} \Delta \dot{S} &= \dot{S}_{\text{out}} + \dot{S}_h - \dot{S}_{\text{in}} - \dot{S}_c = \dot{S}_h - Q_h \left( \frac{\dot{S}}{P} \right)_{\text{out}} \\ &= Q_h \left[ \frac{1}{T} - \left( \frac{\dot{S}}{P} \right)_{\text{out}} \right]. \end{aligned} \quad (39)$$

Here, the irreversibility is considered to be introduced when part of the fluorescence output is turned into heat. The relations between the powers are

$$P_{\text{out}} + Q_h = P_{\text{in}} + Q_c, \quad (40)$$

$$Q_c = \eta_c P_{\text{in}}, \quad (41)$$

$$\frac{P_{\text{out}}}{P_{\text{out}} + Q_h} = \eta_q, \quad (42)$$

where  $\eta_q$  is the luminescence quantum yield. The net cooling power is then the difference between the cooling load and the heat generation, or

$$Q = Q_c - Q_h = P_{\text{in}} [\eta_c - (1 + \eta_c)(1 - \eta_q)], \quad (43)$$

and the cooling coefficient of performance is

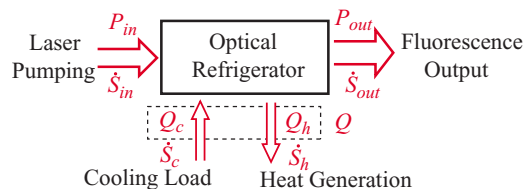


FIG. 11. (Color online) Designation of in and out powers and entropy flow rates. Laser pumping (in), fluorescence output (out), cooling (c), and heat generation (h).



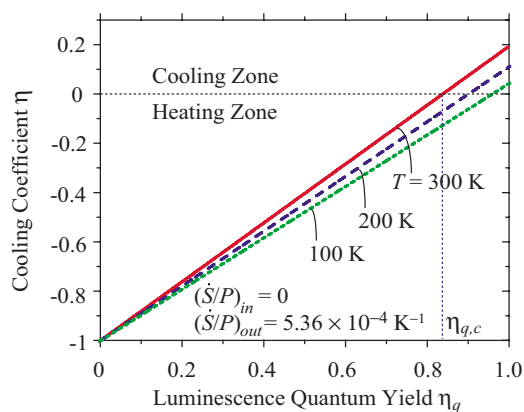


FIG. 12. (Color online) Cooling efficiency as a function of the luminescence quantum yield, for different temperatures.

$$\eta = \frac{Q}{P_{in}} = \eta_c - (1 + \eta_c)(1 - \eta_q). \quad (44)$$

Using Eq. (44) along with Eq. (35), the cooling coefficient may be plotted as a function of the luminescence quantum yield  $\eta_q$ , as shown in Fig. 12. The cooling coefficient has a linear relationship with the luminescence quantum yield. If the luminescence quantum yield is 1, the reversible cycle discussed in the preceding section is recovered, and the cooling coefficient is the Carnot efficiency. In the other extreme, if the luminescence quantum yield is zero, the cooling coefficient becomes  $-1$ , indicating that all the laser pumping energy is turned into thermal energy and deposited into the cooling element. There exists a critical luminescence quantum yield  $\eta_{q,c}$  below which the cooling effect is eliminated. For example,  $\eta_{q,c}$  is 0.83 at room temperature, if the pumping is an ideal laser source and the fluorescence has an entropy flow rate per unit power of  $\dot{S}/P = 5.36 \times 10^{-4} \text{ K}^{-1}$ .

## VII. DISCUSSION

The above analysis indicates that the limiting efficiency of laser cooling of solids can be as high as 20%. However, the

cooling efficiency achieved to date is only around 3%.<sup>19</sup> Hence a significant amount of irreversibility must be present in the experiments. An existing strategy is to use a longer pumping wavelength to obtain higher cooling efficiency, but in practice the absorption coefficient drops more rapidly than the rise in efficiency beyond an optimum detuning. Also, trace impurity absorption eventually dominates over the desired  $\text{Yb}^{3+}$  absorption, causing heating. While the sample could be purified to suppress trace absorption, it seems that new methods would be more useful. For example, the  $\text{Yb}^{3+}$  absorption coefficient could be increased by enhancing the electron-phonon interaction.<sup>20</sup>

The results of this paper show that since current experiments already focus on the use of incident pump sources with zero entropy and spontaneous emission output, no improvements can be expected by resorting to other forms of output. For example, monomode pumping together with random laser output is inherently less efficient than monomode pumping with spontaneous emission output, other things being equal. In the framework of fluorescence, one should explore ion-host combinations which can emit fluorescence with larger entropy flow rate per unit power. Higher luminescence quantum yield is essential, along with higher radiative decay rates (though the latter is only important close to saturation). In summary, improvements are most likely to come from enhanced luminescence quantum yield, enhanced absorption through manipulation of the electron-phonon interaction, improved emission rates, or from altogether new methods.

## ACKNOWLEDGMENTS

One of the authors (S.C.R.) gratefully acknowledges partial support of this research by the Air Force Office of Scientific Research (Contract No. F49620-03-1-0389), and by the National Science Foundation (Grant No. 0502715).

\*Present address: School of Mechanical Engineering, Purdue University, West Lafayette, IN 47907.

†Author to whom all correspondence should be addressed. Electronic address: kaviany@umich.edu

<sup>1</sup>L. Boltzmann, *Lectures on Gas Theory* (Dover, New York, 1995).

<sup>2</sup>C. Shannon, *Bell Syst. Tech. J.* **27**, 379 (1948).

<sup>3</sup>C. Shannon, *Bell Syst. Tech. J.* **27**, 623 (1948).

<sup>4</sup>J. Bekenstein, *Sci. Am.* **15**, 74 (2005).

<sup>5</sup>H. Metcalf and P. van der Straten, *Laser Cooling and Trapping* (Springer-Verlag, New York, 1999).

<sup>6</sup>P. Pringsheim, *Z. Phys.* **57**, 739 (1929).

<sup>7</sup>R. Epstein, M. Buckwald, B. Edwards, T. Gosnell, and C. Mungan, *Nature (London)* **377**, 500 (1995).

<sup>8</sup>S. Vavilov, *J. Phys. (Moscow)* **9**, 68 (1945).

<sup>9</sup>S. Vavilov, *J. Phys. (Moscow)* **10**, 499 (1946).

<sup>10</sup>L. Landau, *J. Phys. (Moscow)* **10**, 503 (1946).

<sup>11</sup>C. Mungan, *Am. J. Phys.* **73**, 1458 (2005).

<sup>12</sup>R. Loudon, *The Quantum Theory of Light* (Oxford University Press, Oxford, 1983).

<sup>13</sup>P. Landsberg and G. Tonge, *J. Appl. Phys.* **51**, R1 (1980).

<sup>14</sup>C. Essex, D. Kennedy, and R. Berry, *Am. J. Phys.* **71**, 969 (2003).

<sup>15</sup>T. Gosnell, *Opt. Lett.* **24**, 1041 (1999).

<sup>16</sup>H. Cao, Y. G. Zhao, S. T. Ho, E. W. Seelig, Q. H. Wang, and R. P. H. Chang, *Phys. Rev. Lett.* **82**, 2278 (1999).

<sup>17</sup>M. Noginov, *Solid State Random Lasers* (Springer, New York, 2005).

<sup>18</sup>M. Kaviany, *Principles of Heat Transfer* (Wiley, New York, 2002).

<sup>19</sup>A. Rayner, N. Heckenberg, and H. Rubinsztein-Dunlop, *J. Opt. Soc. Am. B* **20**, 1037 (2003).

<sup>20</sup>X. Ruan and M. Kaviany, *Phys. Rev. B* **73**, 155422 (2006).